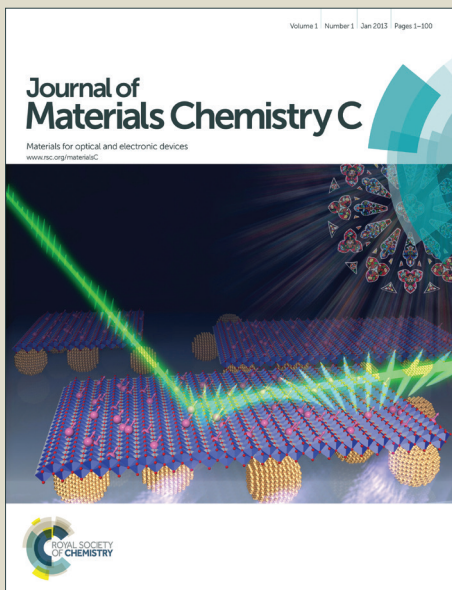


Journal of Materials Chemistry C

Accepted Manuscript



This is an Accepted Manuscript, which has been through the Royal Society of Chemistry peer review process and has been accepted for publication.

Accepted Manuscripts are published online shortly after acceptance, before technical editing, formatting and proof reading. Using this free service, authors can make their results available to the community, in citable form, before we publish the edited article. We will replace this Accepted Manuscript with the edited and formatted Advance Article as soon as it is available.

You can find more information about Accepted Manuscripts in the [Information for Authors](#).

Please note that technical editing may introduce minor changes to the text and/or graphics, which may alter content. The journal's standard [Terms & Conditions](#) and the [Ethical guidelines](#) still apply. In no event shall the Royal Society of Chemistry be held responsible for any errors or omissions in this Accepted Manuscript or any consequences arising from the use of any information it contains.

Cite this: DOI: 10.1039/c0xx00000x

www.rsc.org/xxxxxx

ARTICLE TYPE

An electrodeposited lanthanide MOF thin film as a luminescent sensor for carbonate detection in aqueous solution

Huiping Liu,^a Hongming Wang,^{a,b} Tianshu Chu,^a Minghao Yu^a and Yangyi Yang^{*a}*Received (in XXX, XXX) Xth XXXXXXXXX 20XX, Accepted Xth XXXXXXXXX 20XX*

DOI: 10.1039/b000000x

A luminescent lanthanide MOF-based thin film [$\{[\text{Eu}(\text{HBPTC})(\text{H}_2\text{O})_2]\cdot2\text{DMF}\}_n$] (BPTC = benzophenone-3,3',4,4'-tetracarboxylate) was successfully fabricated by electrodepositing in an anhydride system. In this approach, HO^- anions will accumulate near the cathode while applying a direct current in nitrate solution, followed by benzophenone-3,3',4,4'-tetracarboxylic dianhydride (BTDA) hydrolysis and consequent growth of MOFs directly on electrode surface. The influences of concentration of electrolyte, current density, and conductive salt on the synthesis of the MOF films were investigated. We demonstrate that the carboxylic acid ligands can be replaced by the anhydride to fabricate the lanthanide MOF-based thin film by cathodic electrodeposition. Moreover, photoluminescent properties of this film were investigated and the photoluminescent measurement indicated that this luminescent MOF thin film is a highly selective sensor for carbonate in aqueous solution.

Introduction

Metal-organic frameworks (MOFs) are widely regarded as promising materials for applications in the fields of gas storage, energy storage, separation, catalysis, magnetism, and sensors by controlling the architecture and functionalization of the pores.¹⁻¹¹ Among these, lanthanide metal-organic frameworks (LnMOFs) have emerged as prospective materials for their unique luminescence properties arising from f-f transitions via suitable “antenna effect”, such as larger Stokes shifts, narrow line emission, long luminescence lifetimes and high colour purity.¹²⁻¹⁷ The combination of these inherent luminescent features together with the intrinsic porosity of LnMOFs offers potential for chemical sensing.

The bulk MOFs are generally synthesized by diffusion,³⁰ evaporation, hydrothermal or solvothermal methods and the emerging approach such as microwave¹⁸, ultrasound¹⁹ and electrochemical^{20,21} synthesis. But the brittle crystals or insoluble powders are hard to process with common surface processing techniques and limit the development of MOF. Accordingly, the thin films of MOFs on some substrates have gained attention in recent years. Continuous films are required in various fields, such as the field of gas separation, sensors and catalysis and it is a vital challenge to fabricate thin film structures of MOFs on the desired

substrates. The reported methods for preparing MOF-based thin films can be denoted as seeding-growth^{18,22-25} and functionalization-growth^{26,27} process which may comprise a separated seeding or functionalization and secondary growth step. In addition, layer-by-layer method has been used to fabricate MOF films.²⁸ And a most promising technique to prepare the thin films of MOFs is electrodeposition method due to its mild reaction condition and short reaction time.^{20,29} The electrodeposition can be subdivided into two branches. Firstly, metal ions can be produced in situ by anodic oxidation of a metal support to supply the structural cations for MOFs formation.²⁹⁻³¹ The second approach can be described as cathodic electrodeposition. In contrast to anodic oxidation, cathodic electrodeposition allows accumulation of HO^- anions near the cathode and results in deprotonation of carboxylic acid ligands as reported in the literature,^{32,33} thus confining MOFs crystallization to the electrode. However, to our best knowledge, the studies on this field are limited to transition MOFs, namely MOF-5, HKUST-1, ZIF-8, MIL-100 (Fe), MIL-100(Al), MIL-53(Al), $\text{NH}_2\text{-MIL-53(Al)}$,³⁰⁻³² and there is no correspondingly report about luminescent LnMOF-based thin films prepared by electrodepositing directly.

In the previous work³⁴, a strategy for preparing mechanically robust MOF thin films was developed by electrodepositing of europium hydroxide on ITO in combination with subsequent solvothermal synthesis of MOF films. But the indirect electrochemical deposition technique did not avoid the disadvantages of traditional methods which are time-consuming and power-wasting. In trying to introduce the electrodeposition technique into the field of preparation of LnMOF-based membranes, we noted that anodic oxidation is inapplicable for preparation of LnMOF films due to the chemical instability of

⁴⁰ *MOE Key Laboratory of Bioinorganic and Synthetic Chemistry, KLGHEI of Environment and Energy Chemistry, School of Chemistry and Chemical Engineering, Sun Yat-Sen University, Guangzhou, 510275, P. R. China. E-mail: cesyy@mail.sysu.edu.cn*

^b *Department of Chemistry, Guangdong University of Education, Guangzhou, 510303, P. R. China*

⁴⁵ *†Electronic Supplementary Information (ESI) available: Experimental details and supplementary figures. For ESI see DOI: 10.1039/b000000x/*

lanthanide metals. Hence, cathodic electrodeposition technique has attracted our attention. On the other hand, we were also aware that a certain number of carboxylic acid ligands with large value of dissociation equilibrium constant will coordinate to lanthanide metal ions directly and precipitate from the solution even without adjusting pH of the reaction mixtures or under a low-pH experimental condition, such as oxalic acid and malonic acid. It was adverse to fabricating films on electrode surface.

To address this, we predicted that anhydride or esters will hydrolyze with the rise of concentration of HO^- anions near the cathode result in growth of MOFs. Hence, the carboxylic acid ligands can be replaced by the anhydride or esters. Herein we report on a luminescent LnMOF-based thin film $\left[\{\text{Eu(HBPTC)}(\text{H}_2\text{O})_2\}\cdot 2\text{DMF}\right]_n$ (Eu-HBPTC) (BPTC = benzophenone-3,3',4,4'-tetracarboxylate) that has been prepared by electrodepositing in the mixture of benzophenone-3,3',4,4'-tetracarboxylic dianhydride (BTDA) and $\text{Eu}(\text{NO}_3)_3$. Our results revealed that the dianhydride groups of BTDA were hydrolyzed to tetracarboxylate groups and directly react with europium ion on conductive surface to form the MOFs.

The hydrolysis of BTDA in the reaction solution generates benzophenone-3,3',4,4'-tetracarboxylate (BPTC⁴⁻) along with its different protonation products (HBPTC^{3-} , $\text{H}_2\text{BPTC}^{2-}$, $\text{H}_3\text{BPTC}^{-}$)³⁵. And the aromatic BPTC⁴⁻ possesses several interesting characteristics. It can act not only as hydrogen-bond acceptor but also as hydrogen-bond donor, depending upon the number of protonated carboxyl groups.³⁶ Besides, the complete or partial protonation causes BPTC⁴⁻ rich coordination modes. The structures of Eu-HBPTC were recently reported that the chains of edge-sharing polyhedra are connected into a two-dimensional framework. And the hydrogen bonds between the BPTC⁴⁻ and the water molecules connect the neighbouring layers together into a 3D network. The resulting packing forms a narrow channel to accommodate the solvent molecules.³⁷ However, the study on Eu-HBPTC was limited to investigations of the fundamental synthesis and structural analysis. The detailed spectroscopic analyses, such as excitation spectra and some other functions interrelated with the luminescence spectra, are still unknown.

Indeed, a certain number of LnMOFs are particularly useful to develop new type of sensing materials because of the permanent porosities and collaborative luminescent properties.^{34,38-41} For bulk materials, there are two main methods for luminescent sensing study but with complicated pretreatment. The first method is described as a suspension-state luminescent experiment.⁴⁵ While the second method uses the MOF-ion incorporated samples with an immersion and filtration process to investigate the ionic sensing function of the luminescent MOFs. In comparison, luminescent thin film on an appropriate support material is a convenient method to optically monitor its luminescence intensity as a function of analyte exposure. And the thin film structure on the substrate is benefit for practical sensor applications. We predicted that the metal-organic network thin film (Eu-HBPTC) has potential for acting as a luminescent sensor for selective anion monitoring. The results indicate that this luminescent MOF thin film is a highly selective sensor for carbonate in aqueous solution. And obvious and characteristic colour change from the bright red to colorless can be found when the films were immersed in carbonate aqueous solution under the lab UV lamp

with excitation.

60 Experimental

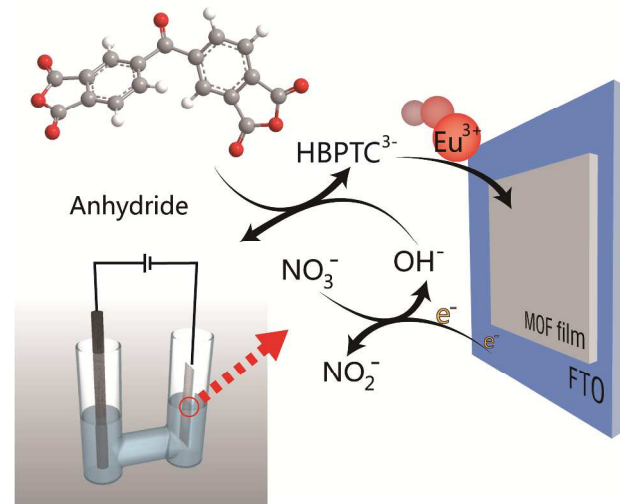
Materials and methods

All chemicals were commercially available and used without further purification. Aqueous solutions of Cl^- , Br^- , I^- , ClO_4^- , BrO_3^- , IO_3^- , HPO_4^{2-} , and CO_3^{2-} were prepared from their potassium salts while PO_4^{3-} , SO_4^{2-} were from their sodium salts. Distilled water was used throughout all experiments.

Morphology and quality of thin films were investigated by using a Hitachi S-4800 Scanning Electron Microscope (SEM), by analyzing both surfaces and cross sections. Electrochemical tests were carried out on a Metrohm PGSTAT 302N electrochemical workstation. The powder X-ray diffraction (PXRD) patterns were obtained using a Bruker D8 Advance equipped with Cu K α radiation ($\lambda=1.5418 \text{ \AA}$) at a scanning rate of $2^\circ \cdot \text{min}^{-1}$ with 20 ranging from 5 to 50° . FT-IR spectra were recorded from KBr pellets in the range of $4000\text{--}400 \text{ cm}^{-1}$ on a Nicolet 330 FT-IR spectrometer. Absorption spectra of these samples were recorded on an UV-Vis-NIR spectrophotometer (UV3150, Shimadzu), and the scan speed was fixed at $5 \text{ nm} \cdot \text{s}^{-1}$. Luminescence spectra were collected by a RF-5301PC luminescence spectrometer. And all the measurements were carried out at room temperature (298 K).

Synthesis of Eu-HBPTC powder

As reported in the literature³⁷, the powder of Eu-HBPTC was prepared as follows: 32 mg (0.1 mmol) benzophenone-3,3',4,4'-tetracarboxylic dianhydride (BTDA), 45 mg (0.1 mmol) europium nitrate hexahydrate and demineralized 2 mL water were placed in a 10 mL Teflon-lined stainless-steel vessel and heated at 180°C for 3 days under autogenous pressure. After the reaction mixture was cooled down to room temperature, the powder of Eu-HBPTC were filtered off, washed with distilled water, and dried in air.



Scheme 1 General scheme for the cathodically induced electrodeposition of MOFs, involving the reduction of nitrate and generation of HO^- (A), the hydrolysis of anhydride (BTDA)(B), and MOF crystallization from HBPTC^{3-} and Eu^{3+} (C).

Electrodeposition of Eu-HBPTC thin films

Fluorine-doped Tin Oxide conductive glass (FTO, about $25 \times 10 \text{ mm}^2$) was cleaned by ultrasound in acetone, ethanol and distilled water for 20 minutes separately.⁴² 64 mg (0.2 mmol) benzophenone-3,3',4,4'-tetracarboxylic dianhydride (BTDA) was dissolved in 10 mL DMF, and then 9 mg (0.2 mmol) $\text{Eu}(\text{NO}_3)_3 \cdot 6\text{H}_2\text{O}$ was dissolved in the solution. The mixture was stirred in a magnetic agitator for 30 minutes.

The electrodeposition process of Eu-HBPTC was carried out in the mixture by applying a constant current density of $0.4 \text{ mA} \cdot \text{cm}^{-2}$ with a potentiostat for 10 minutes. A classic two-electrode cell was employed with graphite rod as the anode and the FTO conductive glass as the cathode (Scheme 1). The films were washed with distilled water, and dried in air. Beside, in trying get better morphology and quality of thin films, the thin films were prepared by electrodepositing for 10 minutes and treated hydrothermally at 180°C for 72 hours.

Results and discussion

Optimization of fabrication condition of the films

For comparison purposes, electrochemical depositions were formed at various current densities ($0.3 \sim 1.5 \text{ mA} \cdot \text{cm}^{-2}$) and concentration of reaction solution ($0.005 \text{ M} \sim 0.1 \text{ M}$, both of BTDA and $\text{Eu}(\text{NO}_3)_3$). A higher concentration of europium ions and BTDA in the electrolyte may shorten the incubation period of the coordination reaction. But an increased concentration of reactants is not always better; a higher concentration of BTDA will lead to a higher viscosity of the solution because of the $\pi \cdot \pi$ stacking interaction between the aromatic groups of BTDA²⁰, which will cause the conductivity of the solution to decrease. In addition, it is well known to us that the conductivity of electrolyte solution increases with the increase of the concentration in a certain concentration range but shows the opposite when in a higher range. The increased interaction between positive and negative ions results in the reduction of migration rate of ions and conductivity of bath solution. The result indicated that the higher concentration of reaction solution, the higher current density was required to get the film on FTO in a certain interval of time. For example, the films could be obtained at $0.3 \text{ mA} \cdot \text{cm}^{-2}$ in the mixture containing 0.01 M BTDA and 0.01 M $\text{Eu}(\text{NO}_3)_3$ while the films could not be observed on top of FTO in 0.05 M reagents until the current density increased to $1.2 \text{ mA} \cdot \text{cm}^{-2}$. It is probably because of the decrease of the conductivity of bath solution with the increase of concentration. Consequently, current efficiency will be greatly reduced.

Besides, even though a layer was formed on top of the FTO, the qualities of films and the adhesion of the MOF to the surface were different from case to case. The films obtained with a higher current density only partially covered by MOF and can be washed off just by rinsing with water. Furthermore, in order to raise the conductivity, some conductive salt like NH_4NO_3 was added into reaction solution. However, the FTO surface was also only partially covered by MOF along with flocculent deposit in the solution. And so did cetyltrimethylammonium bromide (CTAB), tetrabutylammonium bromide (TBAB) and sodium dodecyl sulfate (SDS). But on the contrary, if conductive salt was absent in the electrolytic bath, better films were obtained and no

suspended material was found in the solution.

Inspired by these and took the factors into account, the films were obtained using a current density of $0.4 \text{ mA} \cdot \text{cm}^{-2}$ and the reaction solution containing 0.02 M $\text{Eu}(\text{NO}_3)_3$ and 0.02 M BTDA for further studies.

Possible mechanism of electrodeposition

The mechanism of cathodic electrodeposition of MOFs has been reported recently and the mechanism also applies to this work but with little modulation.^{32,33}

Cyclic voltammogram (CV) of the mixture of 0.02 M $\text{Eu}(\text{NO}_3)_3$ and 0.02 M BTDA in DMF was obtained using FTO working electrodes and referenced against a saturated calomel electrode (SCE). To illustrate how deposition works, the CVs of 0.02 M $\text{Eu}(\text{NO}_3)_3$, BTDA, DMF were obtained as well.

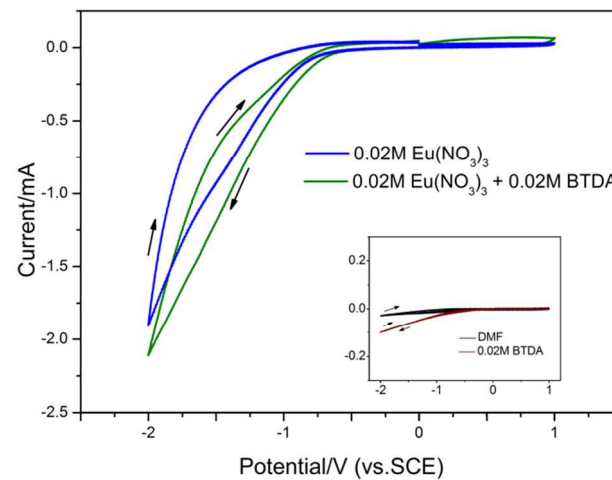
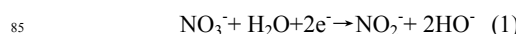


Fig. 1 Cyclic voltammograms of different solutions in DMF obtained using FTO working electrodes at scan rate of $100 \text{ mV} \cdot \text{s}^{-1}$. The inset shows CVs of a 0.02 M BTDA solution and DMF using FTO working electrode.

As shown in Fig. 1, at a scan rate of $100 \text{ mV} \cdot \text{s}^{-1}$, a reduction from the mixture containing $\text{Eu}(\text{NO}_3)_3$ and BTDA was observed at approximately -0.7 V (vs. SCE) as well as the solution of $\text{Eu}(\text{NO}_3)_3$. In contrast, the onset of reduction did not occur in the solution of BTDA or DMF. We suspected that it was the reduction of NO_3^- occurs on FTO shown as below.⁴³ The reduction was subsequently indicated by Griess reagent, which tested positive for the presence of NO_2^- in the postelectrolytic deposition solution as reported in the literature.³²



It is reasonable to surmise that the thin films of Eu-HBPTC were deposited at the cathode through a mechanism of electrochemical generation of base in nitrate solution,⁴⁴ according to the reaction (1) which caused the local increase of concentration of HO^- and led close to cathodic area to the BTDA hydrolysis and consequent growth of MOFs directly on FTO surface, as shown in Scheme 1.

We also succeeded in preparing the thin films of Tb-HBPTC and Gd-HBPTC under the similar condition but without further research.

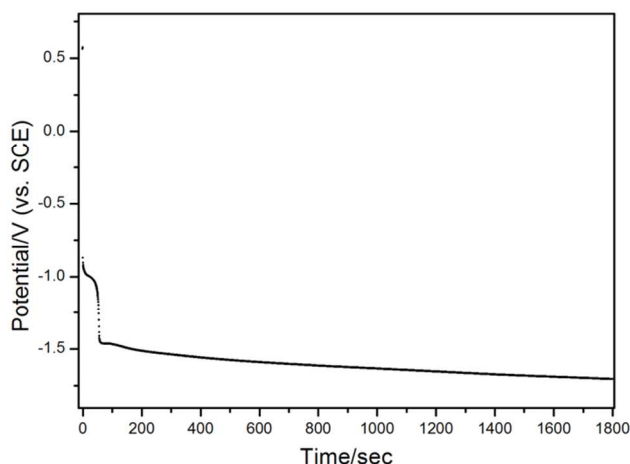


Fig. 2 Potential (vs. SCE) versus time curve during the electrodeposition of Eu-HBPTC films at constant current density. The experiment was carried out at $0.4 \text{ mA} \cdot \text{cm}^{-2}$ in the mixture containing $0.02 \text{ M} \text{ Eu}(\text{NO}_3)_3$ and $0.02 \text{ M} \text{ BTDA}$ at 298 K .

As shown in Fig. 2, after an initial voltage drop from the open circuit potential to -0.87 V (vs. SCE), the electrode potential decreases slowly at the very beginning and then dropped drastically to -1.45 V at about 1 min. It is worth pointing out that the thin film on FTO was observed which caused the sudden increase of resistance and we name it the first layer. The NO_3^- reduction occurs on the first layer which requires large overpotentials and causes the growth of Eu-HBPTC.³² And then the electrode potential decreases almost linearly during the electrodeposition process. The increasing overvoltage that illustrates the process is presumably related to the thickening of the deposits.⁴³

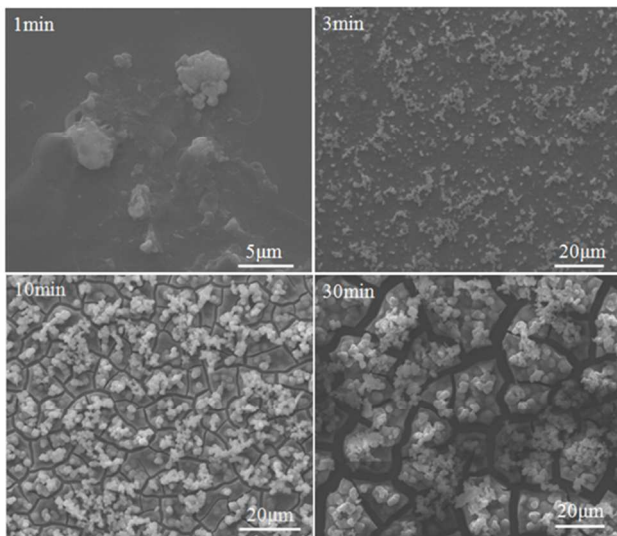


Fig. 3 Top-down SEM micrographs of the chapped films at different time intervals.

In order to have an intuitive observation of the variation of surface morphology and thickness, the chapped thin films were obtained by drying at 60°C to accelerate the volatilization of solvent molecules. The morphology and structure of the chapped

films were monitored by scanning electron microscopy (SEM) at different time intervals as shown in Fig. 3. Figure 3 indicates that a uniform layer was formed along with some protuberant mound-like patches of Eu-HBPTC (second layer) in 1 minute. This means that the first layer of films coated the FTO surface along with a secondary growth. Over time the density and thickness of the films obviously increases. After 30 minutes, the second layer grows bigger and more intergrown. Apparently, the speculation is confirmed by the SEM. Longer reaction times resulted in thicker films as well as the diameters of the second layer. The thickness of the film prepared by applying constant current for 10 min is about $1 \mu\text{m}$ (Fig. S1†) and it is thick enough for luminescent properties researches and sensing studies.

Surprisingly, the films with better morphology and crystallization were obtained by treating hydrothermally at 180°C for 72 hours. As shown in Fig. 4 (left), top-down views of the film show the patches of Eu-HBPTC petals with "microflower" morphology. Meanwhile, cross-sectional SEM image (Fig. 4, right) of the film shows excellent coverage of the substrate with a 500 nm thick layer. Fortunately, the films, no matter treated hydrothermally or not, would not drop off in water over several weeks, indicating that the films combined with the FTO glass firmly.

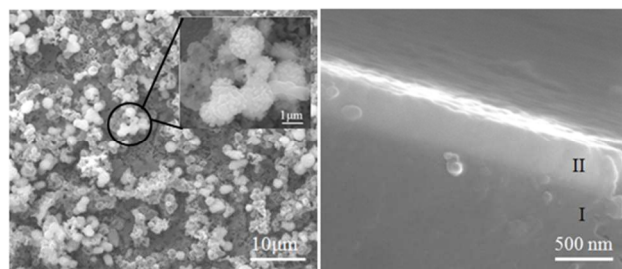


Fig. 4 (left) Top-down SEM images of the film after treating hydrothermally and (right) cross-sectional SEM showing the thickness of the this film (I, FTO glass substrate; II, Eu-HBPTC MOF film).

Powder X-ray diffraction and FT-IR analyses

The PXRD pattern (Fig. S2†) of Eu-HBPTC prepared by the electrodepositing is similar to that of Eu-HBPTC synthesized through the reported method. And it illustrates that Eu-HBPTC films can be prepared by the electrochemical method. However, the XRD patterns show poor crystallinity but generally matches the theoretical spectrum.^{37,45} Lack of crystallinity could be due to film drying before or during XRD analysis, leading to film degradation.²³ Attempts to improve crystallinity of Eu-HBPTC films and powder have thus far been unsuccessful.

The IR spectra of Eu-HBPTC films and Eu-HBPTC prepared through hydrothermal method are shown in Fig. S3(ESI†). The peak shapes and positions in the three spectra are similar, further illustrating that Eu-HBPTC films were successfully synthesized by electrodepositing. The characteristic bands of the carboxylate groups within the solids are presented around 1548 cm^{-1} for the asymmetric stretching vibration $\nu_{as}(\text{COO})$ and 1413 cm^{-1} for the symmetric stretching vibration $\nu_s(\text{COO})$. Other characteristic bands range from $854\text{--}667 \text{ cm}^{-1}$ of the C-H vibration have also been observed.

Photoluminescent properties of Eu-HBPTC films

The excitation and emission spectra of Eu-HBPTC-based thin films were recorded at room temperature (298 K). As indicated in the excitation spectra of the 617 nm emission for films in air (Fig. 5), the strong, broad band centred at about 317 nm is observed, which is ascribed to the $\pi-\pi^*$ electron transition of the organic ligands. Additionally, the maximal band in the excitation spectrum of films in water (Fig. 5) is 317 nm as well but little weaker than in air due to the influence of water. The emission spectra of films both in air and in water have identical profile. The emission spectra centred at 581, 594, 617, 653, 700 nm can be seen, which correspond to ${}^5D_0 \rightarrow {}^7F_J$ ($J = 0 \rightarrow 4$) transitions of Eu^{3+} ions, respectively.^{34,46} The symmetric forbidden emission band of ${}^5D_0 \rightarrow {}^7F_0$ around 581 nm is weak; the medium-strong emission around 594 nm is attributed to the magnetic dipolar ${}^5D_0 \rightarrow {}^7F_1$ transition and the strongest emission peak around 617 nm is ascribed to the electric-dipolar ${}^5D_0 \rightarrow {}^7F_2$ transition. In addition, the weak emission peaks at 653 nm (${}^5D_0 \rightarrow {}^7F_3$) and 700 nm (${}^5D_0 \rightarrow {}^7F_4$) also correspond to magnetic dipole transitions.^{34,46} The strong emission in water means it has the potential to be a new type of sensing materials for the sensing of ions in aqueous solution.

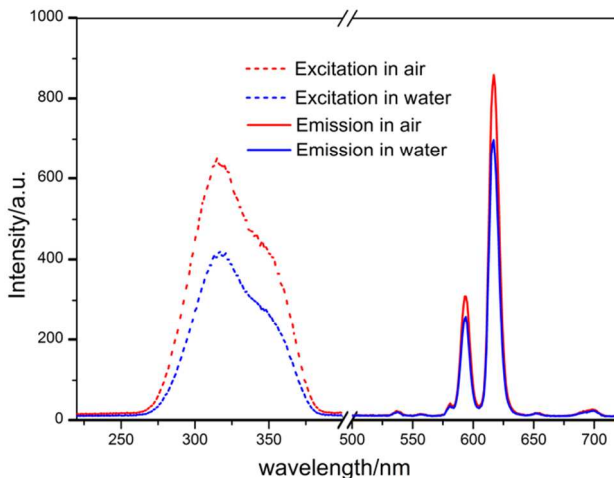


Fig. 5 Excitation and emission curve of the films in air or water, respectively.

Photoluminescent sensing study of Eu-HBPTC films in aqueous solution

Taking advantage of the property and structure of Eu-HBPTC, a further research for sensing anions in aqueous solution was undertaken. It is necessary to point out that the emission spectra of the films discussed below were all excited at 317 nm. Before the sensing study, in order to investigate the luminescent properties of the thin films in different media, the time-dependent emission intensity of the films in the presence of different media at 298 K was monitored shown in Fig. 6. The emission intensity at 617 nm of thin film decreased by about 24% in 80 minutes and then remained stable. We suspected that the films were prepared in DMF solution and the channel of the compounds were filled with DMF molecules. However, the DMF were expelled out of the channel by H_2O molecules when the films were immersed in water. Water molecules bound to LnMOFs will limit the emission efficiency due to vibrational quenching process.⁴⁷ And this

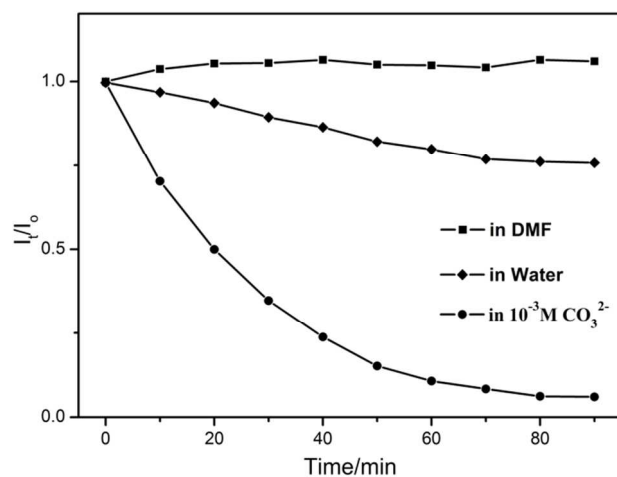


Fig. 6 Dependence of the ratio I_t/I_0 of Eu-HBPTC films versus time in DMF (top), water (middle) and $10^{-3} \text{ M } \text{CO}_3^{2-}$ solution at 298 K (excited at 317 nm). I_t and I_0 are the intensities of the ${}^5D_0 \rightarrow {}^7F_2$ transition (at 617 nm) of film at time t and at the time when the film was just immersed in the solution, respectively.

exchange reached the point-of-equivalence, where no more spectral changes occurred after 80 minutes. The emission intensity in DMF showed no significant change with the extension of the time that confirmed the hypothesis.⁴⁸ Took this factor into account, the thin films for luminescent sensing study were immersed in water for 2 hours before detection of anions in aqueous solution. Moreover, when the pre-treated film was immersed in $10^{-3} \text{ M } \text{CO}_3^{2-}$ for two hours, the luminescence almost disappeared. It is reasonable to determine to expose the film in the analyte for 2 hours.

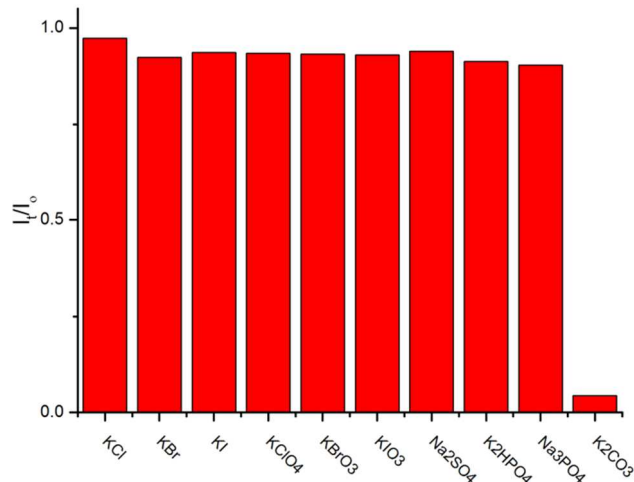


Fig. 7 Diagrams of the ratio I_t/I_0 of Eu-HBPTC films in different 10^{-3} M anions aqueous solution when excited at 317 nm (298 K). I_t and I_0 are the intensities of the ${}^5D_0 \rightarrow {}^7F_2$ transition (at 617 nm) of film at time t (2 h) and at the time when the film was just immersed in the solution, respectively.

To demonstrate the feasibility for anion sensing, emission spectra of pre-treated films with the thickness of about 1 μm were in situ recorded in various anions aqueous solutions. The

photoluminescence responses of the pre-treated thin films for the various anions aqueous solutions are shown in Fig. 7 and Fig. S4(ESI†). We observe the drastic reduction of the strongest emission of Eu³⁺ ($^5D_0 \rightarrow ^7F_2$, 617 nm) for the CO₃²⁻ anion, whereas SO₄²⁻, PO₄³⁻, HPO₄²⁻, ClO₄⁻, BrO₃⁻, IO₃⁻ and halide ions show no significant change under the same experimental conditions. It is worth to note that the film immersed in CO₃²⁻ for 2 hours shows no luminescence under the lab UV lamp (254 and 365 nm) or under a handy UV banknote detector with excitation that can be distinguished by naked eyes (Fig. S5†). And it can be used as a convenient sensor simply coupled with a handy UV cash detector to detect CO₃²⁻. In trying to demonstrate the ability of films for detection of carbonate in aqueous solution, fluorescence quenching experiments were performed through adding CO₃²⁻ aqueous solutions with different concentrations. As shown in Fig. 8, the decrease of fluorescence intensity is evident after adding the aqueous solution of CO₃²⁻. Upon the addition of 10⁻³ M aqueous solution of CO₃²⁻, the fluorescence intensity was almost quenching. Meanwhile, luminescence intensity of Eu-HBPTC immersed in a 10⁻⁴ M CO₃²⁻ aqueous solution is more than 2 times weaker than that of non CO₃²⁻ incorporated, which means that the high sensitivity can be applied to easily identify the existence of a small amount of CO₃²⁻ in aqueous solution.

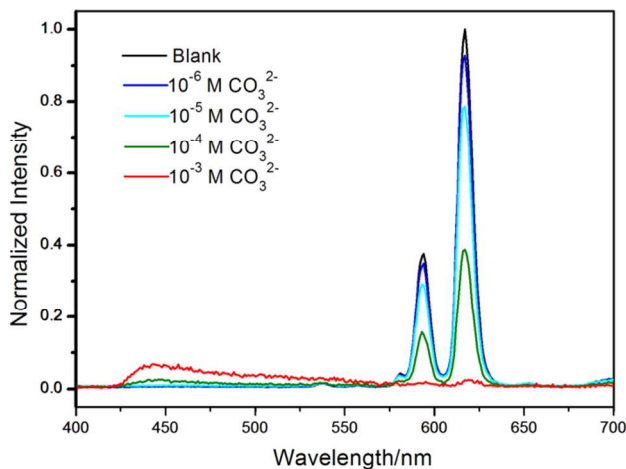


Fig. 8 Emission spectra of the film after being immersed in CO₃²⁻ aqueous solution at various concentrations at 298 K (excited at 317 nm). The data were normalized to the intensity of the blank sample.

Mechanism for quenching effect of carbonate on the fluorescence of Eu-HPTC film is of interest to us. Based on the reported LnMOF sensors, luminescence modulation can be induced through three main mechanisms.⁴⁹ Firstly, one may act directly onto the trivalent lanthanide ion by displacing the small coordinated molecules, such as water molecule. Secondly, one may influence the photophysical properties of the ligand, either of its singlet state or of its triplet state. Thirdly, the analyte itself may be used as either sensitising moiety for the trivalent lanthanide ion luminescence or possibly as a quencher if there was an unsaturated coordination environment. Obviously, it cannot be the first mechanism. If the coordinated water molecules of Eu-HBPTC are displaced by CO₃²⁻, the luminescent intensity will increase rather than quench due to the notorious action of

water molecule as a photoluminescence quencher.⁴⁷ It cannot be the third mechanism either because there is no spare coordination site for CO₃²⁻. Consequentially, it is likely to follow the second mechanism. The UV–Vis absorbance of carbonate and Eu-HBPTC aqueous solution indicates that CO₃²⁻ did not affect the absorbance of Eu-HBPTC (Fig. S6†). And as indicated in the emission spectra of the film immersed in a 10⁻⁴ M CO₃²⁻ aqueous solution in Fig. 8, a distinct broad band range from 425 to 460 nm is observed, which is ascribed to the fluorescence of ligands.⁵⁰ In addition, the intensity of the band is increase with the increase of the carbonate concentration. It indicates that the energy transfer from the organic ligands to Eu³⁺ ions is not efficient with the influence of carbonate. Oppositely, the band cannot be observed in the emission spectra of the film immersed in other anions (Fig. S4†).

These confirm our speculation that carbonate may influence the photophysical properties of the ligand with a binding process to the protonated carboxyl groups, affecting the rate of energy transfer onto the europium ion, henceforth the luminescence intensity. Moreover, we surmised that it needs to comply with at least two requirements for triggering the fluorescence quenching. On one hand, the quencher should have an appropriate size for getting into the narrow channel of Eu-HBPTC; on the other hand, the quencher should be with some binding ability to the ligands.^{39,51} Evidently, the carbonate meets the two requirements. In contrast, the anions with bigger size (SO₄²⁻, PO₄³⁻, HPO₄²⁻, ClO₄⁻, BrO₃⁻, IO₃⁻) or weaker binding ability (Cl⁻, Br⁻, I⁻) do not affect the “antenna effect”. The behaviours of these anions and quenching mechanism will be further investigated.

Conclusions

In conclusion, the Eu-HBPTC-based MOF thin film was successfully fabricated by electrodepositing in an anhydride system. In this approach, HO⁻ anions accumulate near the cathode while apply a direct current in nitrate solution, and cause benzophenone-3,3',4,4'-tetracarboxylic dianhydride (BTDA) hydrolysis, followed by coordinating with europium ion and growth of Eu-HBPTC on FTO surface. The LnMOF film was characterized by SEM, PXRD and FT-IR; it exhibits a high stability in aqueous solution with high luminescence intensity. Moreover, an obvious luminescence quenching of the film was observed for CO₃²⁻ aqueous solution while other anions show no significant change in the same conditions, indicating that this LnMOF thin film is a highly selective sensor for carbonate in aqueous solution. The application of this carbonate sensor in biological systems is proceeding.

Acknowledgements

The authors acknowledge the financial support of the National Natural Science Foundation of China (50572125, 20973203 and 91022012) and the Fundamental Research Funds for the Central Universities.

References

1. H. Furukawa, K. E. Cordova, M. O'Keeffe and O. M. Yaghi, *Science*, 2013, **341**, 1230444.

2. J. Park, H. Kim and Y. Jung, *The J. Phys. Chem. Lett.*, 2013, **4**, 2530-2534.
3. M. Zhang, G. Feng, Z. Song, Y. P. Zhou, H. Y. Chao, D. Yuan, T. T. Tan, Z. Guo, Z. Hu, B. Z. Tang, B. Liu and D. Zhao, *J. Am. Chem. Soc.*, 2014, **136**, 7241-7244.
4. C. M. Doherty, D. Buso, A. J. Hill, S. Furukawa, S. Kitagawa and P. Falcaro, *Acc. Chem. Res.*, 2014, **47**, 396-405.
5. Z.-Y. Gu, J. Park, A. Raiff, Z. Wei and H.-C. Zhou, *ChemCatChem.*, 2014, **6**, 67-75.
10. 6. A. Wild, A. Winter, M. D. Hager and U. S. Schubert, *Analyst*, 2012, **137**, 2333-2337.
7. J. X. Zhang, H. Li, C. F. Chan, R. Lan, W. L. Chan, G. L. Law, W. K. Wong and K. L. Wong, *Chem. Commun.*, 2012, **48**, 9646-9648.
8. X. Yan, X. Li, Z. Yan and S. Komarneni, *Appl. Surf. Sci.*, 2014, **308**, 306-310.
15. 9. F. Cacho-Bailo, B. Seoane, C. Téllez and J. Coronas, *J. Membrane Sci.*, 2014, **464**, 119-126.
10. R. Kumar, K. Jayaramulu, T. K. Maji and C. N. Rao, *Chem. Commun.*, 2013, **49**, 4947-4949.
20. 11. Y. Cui, Y. Yue, G. Qian and B. Chen, *Chem. Rev.*, 2012, **112**, 1126-1162.
12. M. D. Allendorf, C. A. Bauer, R. K. Bhakta and R. J. Houk, *Chem. Soc. Rev.*, 2009, **38**, 1330-1352.
13. Z. Dou, J. Yu, Y. Cui, Y. Yang, Z. Wang, D. Yang and G. Qian, *J. Am. Chem. Soc.*, 2014, **136**, 5527-5530.
25. 14. L. Armelao, G. Bottaro, S. Quici, M. Cavazzini, M. C. Raffo, F. Barigelli and G. Accorsi, *Chem. Commun.*, 2007, 2911-2913.
15. C.-H. Zeng, J.-L. Wang, Y.-Y. Yang, T.-S. Chu, S.-L. Zhong, S. W. Ng and W.-T. Wong, *J. Mater. Chem. C*, 2014, **2**, 2235-2242.
30. 16. Y. Zheng, C. Tan, Q. Wang and C. C. Zhang, *Solid State Sci.*, 2011, **13**, 1687-1691.
17. G. L. Law, W. M. Kwok, W. T. Wong, K. L. Wong and P. A. Tanner, *J. Phys. Chem. B*, 2007, **111**, 10585-10861.
18. Y. Yoo and H. K. Jeong, *Chem. Commun.*, 2008, 2441-2443.
35. 19. M. A. Alavi and A. Morsali, *Ultrason. Sonochem.*, 2014, **21**, 674-680.
20. H. M. Yang, X. L. Song, T. L. Yang, Z. H. Liang, C. M. Fan and X. G. Hao, *RSC Adv.*, 2014, **4**, 15720-15726.
21. R. Ameloot, L. Stappers, J. Fransaer, L. Alaerts, B. F. Sels and D. E. De Vos, *Chem. Mater.*, 2009, **21**, 2580-2582.
40. 22. Y. Mao, W. Cao, J. Li, L. Sun and X. Peng, *Chem.-Eur. J.*, 2013, **19**, 11883 - 11886.
23. Y. Abdollahian, J. L. Hauser, I. R. Colinas, C. Agustin, A. S. Ichimura and S. R. J. Oliver, *Cryst. Growth Des.*, 2014, **14**, 1506-1509.
45. 24. K. Khaletskaya, S. Turner, M. Tu, S. Wannapaiboon, A. Schneemann, R. Meyer, A. Ludwig, G. Van Tendeloo and R. A. Fischer, *Adv. Funct. Mater.*, 2014, DOI: 10.1002/adfm.201400559.
25. T. T. Tan, M. R. Reithofer, E. Y. Chen, A. G. Menon, T. S. Hor, J. Xu and J. M. Chin, *J. Am. Chem. Soc.*, 2013, **135**, 16272-16275.
50. 26. M. T. Conato and A. J. Jacobson, *Microporous Mesoporous Mater.*, 2013, **175**, 107-115.
27. D. Zacher, A. Baunemann, S. Hermes and R. A. Fischer, *J. Mater. Chem.*, 2007, **17**, 2785-2792.
28. A. R. Abbasi, K. Akhbari and A. Morsali, *Ultrason. Sonochem.*, 2012, **19**, 846-852.
55. 29. T. R. C. Van Assche, G. Desmet, R. Ameloot, D. E. De Vos, H. Terryn and J. F. M. Denayer, *Microporous Mesoporous Mater.*, 2012, **158**, 209-213.
30. N. Campagnol, T. Van Assche, T. Boudewijns, J. Denayer, K. Binnemans, D. De Vos and J. Fransaer, *J. Mater. Chem. A*, 2013, **1**, 5827-5830.
31. A. Martinez Joaristi, J. Juan-Alcañiz, P. Serra-Crespo, F. Kapteijn and J. Gascon, *Cryst. Growth Des.*, 2012, **12**, 3489-3498.
32. M. Li and M. Dincă, *J. Am. Chem. Soc.*, 2011, **133**, 12926-12929.
33. M. Li and M. Dincă, *Chem. Sci.*, 2014, **5**, 107-111.
34. Y.-M. Zhu, C.-H. Zeng, T.-S. Chu, H.-M. Wang, Y.-Y. Yang, Y.-X. Tong, C.-Y. Su and W.-T. Wong, *J. Mater. Chem. A*, 2013, **1**, 11312-11319.
35. H.-Y. Lin, B. Mu, X.-L. Wang and A.-X. Tian, *J. Organomet. Chem.*, 2012, **702**, 36-44.
36. R. Cao, D. F. Sun, Y. C. Liang, M. C. Hong, K. Tatsumi and Q. Shi, *Inorg. Chem.*, 2002, **41**, 2087-2094.
37. P. Thuéry and B. Masci, *CrystEngComm.*, 2010, **12**, 2982-2988.
38. H. M. Wang, Y. Y. Yang, C. H. Zeng, T. S. Chu, Y. M. Zhu and S. W. Ng, *Photochem. Photobiol. Sci.*, 2013, **12**, 1700-1706.
39. K. L. Wong, G. L. Law, Y. Y. Yang and W. T. Wong, *Adv. Mater.*, 2006, **18**, 1051-1054.
40. H. M. Wang, H. P. Liu, T. S. Chu, Y. Y. Yang, Y. S. Hu, W. T. Liu and S. W. Ng, *RSC Adv.*, 2014, **4**, 14035-14041.
41. C. H. Zeng, Y. Y. Yang, Y. M. Zhu, H. M. Wang, T. S. Chu and S. W. Ng, *Photochem. Photobiol.*, 2012, **88**, 860-866.
42. H. Wang, R. Liu, L. Liu, X. Shi and Z. Xu, *Electrochim. Commun.*, 2012, **17**, 79-81.
43. P. Bocchetta, M. Santamaria and F. Di Quarto, *Electrochim. Commun.*, 2007, **9**, 683-688.
44. G. H. A. Therese and P. V. Kamath, *Chem. Mater.*, 1999, **11**, 3561-3564.
45. X. Fan, S. Freslon, C. Daiguebonne, G. Calvez, L. Le Pollès, K. Bernot and O. Guillou, *J. Mater. Chem. C*, 2014, **2**, 5510-5525.
46. 90. W. S. Lo, W. M. Kwok, G. L. Law, C. T. Yeung, C. T. Chan, H. L. Yeung, H. K. Kong, C. H. Chen, M. B. Murphy, K. L. Wong and W. T. Wong, *Inorg. Chem.*, 2011, **50**, 5309-5311.
47. Q. B. Bo, H. T. Zhang, H. Y. Wang, J. L. Miao and Z. W. Zhang, *Chem.-Eur. J.*, 2014, **20**, 3712-3723.
48. Y. Li, S. Zhang and D. Song, *Angew. Chem., Int. Ed. Engl.*, 2013, **52**, 710-713.
49. J. C. Bunzli and C. Piguet, *Chem. Soc. Rev.*, 2005, **34**, 1048-1077.
50. Y.-N. Zhang, H. Wang, J.-Q. Liu, Y.-Y. Wang, A.-Y. Fu and Q.-Z. Shi, *Inorg. Chem. Commun.*, 2009, **12**, 611-614.
51. J. Vanek, P. Lubal, P. Hermann and P. Anzenbacher, Jr., *J. fluoresc.*, 2013, **23**, 57-69.

Graphical Abstract

A luminescent lanthanide MOF-based thin film was fabricated by electrodepositing in an anhydride system and this film can be used as a highly selective sensor for CO_3^{2-} in aqueous solution.

